Allam et al. 2017. *Int. J. Vehicle Structures & Systems*, 9(2), 117-123
ISSN: 0975-3060 (Print), 0975-3540 (Online)
doi: 10.4273/ijvss.9.2.11

International Journal of Vehicle Structures & Systems
Available online at www.maftree.org/eja

Effect of Active Roll Stabilizer System Performance on Vehicle Stability

Essam M. Allam and M.A.A. Emam[a]

Dept. of Automotive and Tractors Engg., Helwan University, Cairo, Egypt
[a]Corresponding Author, Email: mohemam_70@yahoo.com

ABSTRACT:

To investigate the effect of active roll stabilizer system performance on vehicle stability, it is needed to study the effects of varying speeds of the on-road vehicles under different wheel steer angle on the roll angle, side slip angle and yaw rate on the vehicle stability. For a safe drive, when a vehicle is cornering it should not lose its stability on road. In this paper the response of passive and active roll stabilizer vehicle systems are simulated and compared against each other. The results of the simulation model showed a significant influence of the vehicle speed on the vehicle stability under different wheel steer angles.

KEYWORDS:

Active anti-roll bar; Vehicle stability; Passive and active roll stabilizer; MATLAB Simulink; Steer angles

CITATION:

E.M. Allam and M.A.A. Emam. 2017. Effect of Active Roll Stabilizer System Performance on Vehicle Stability, *Int. J. Vehicle Structures & Systems*, 9(2), 117-123. doi:10.4273/ijvss.9.2.11.

NOMENCLATURE:

θ	*Pitch angle of vehicle body state space variable*
ϕ	*Roll angle of vehicle body state space variable*
Z	*Vertical displ. of vehicle body state space variable*
β	*Side slip angle state space variable*
ψ	*Yaw angle state space variable*
z_{ui}	*Vertical displ. of unsprung mass state space variable*
z_{oi}	*Road disturbance displacement input*
V	*Vehicle speed input m/s*
δ	*Wheel steer angle state space variable*
δ_{sw}	*Steering wheel angle input rad*
i_s	*Steering ratio*
S_i	*Cornering force state space variable*
M_{zi}	*Aligning torque state space variable*
W_i	*Vertical load state space variable*
Ki	*Cornering stiffness state space variable*
β_I	*Side slip angle of tire state space variable*
F_{zi}	*Vertical force from suspension state space variable*
x_{sti}	*Suspension stroke state space variable*
$F_{antirolli}$	*Vertical force from anti-roll bar state space variable*
P_i	*Dynamic fluct. of vert. load state space variable*
x_{ti}	*Deflection of tire state space variable*
suffix f,r	*Front, rear*
suffix 1,2	*Front-left wheel, front-right wheel*
suffix 3,4	*Rear-left wheel, rear-right wheel*
μ	*Road friction coefficient*

1. Introduction

Any vehicle mainly runs on three axes of motion (lateral, vertical and longitudinal) and the rotational motions about these axes are called pitch, yaw and roll respectively. The ride comfort and safety are affected by the movements and accelerations of the vehicles caused by pitch and roll motions. Vehicle rollover is considered as one of the most significant causes of injuries and fatalities in road accidents. Thus, the researchers have been interested in changing, developing or modifying in the vehicle design to prevent rollover [1-2]. The passive anti-roll bar is deformed when right and left suspensions are moving oppositely. However, the linkages of the right and left wheels introduce a coupling between suspensions, and transfer a disturbance from one side to the other one. The solution is based on an active anti-roll bar and equipped with the active control system for vehicle stability [3].

Some researchers [4-5] studied the basics of vehicle dynamics by considering two axle vehicles. The characteristics of the suspension systems and handling of the vehicles were analyzed in a steady state and transient manoeuvres for simplified models by using simulation of multi body dynamics of road vehicles [6-9]. The influencing parameters on the rollover tendency and investigation of active suspension control by using simulation model compared with the experimental results on rollover of passenger vehicles were reported in [10-12]. The active (electric) stabilizer bar has a smaller roll angle in the same lateral acceleration when compared to passive stabilizer bar which means a better roll stability [13]. When the vehicle is subjected to a lateral acceleration due to centrifugal or gravitational forces, the active anti-roll bar (AARB) works against any non-symmetric movements between the left and right suspensions is used during a steady turning motion and even on an inclined road surface [3].

2. Modeling and simulation

The simulation is carried out to compare the response of passive, active systems and the failure condition of the active system using Simulink model. Fig. 1 and 2 show a four wheeled full vehicle model and its Simulink model respectively. In order to compare the response of a passive anti-roll bar with an active one equipped in a vehicle, a full vehicle four wheeled model which has nine degrees of freedom with the parameters as given in

Table 1 is used. The full car model equations of motion are as follows:

$$m_s\ddot{Z} = F_{z1} + F_{z2} + F_{z3} + F_{z4} \quad (1)$$

$$F_{z1} = k_1 \cdot x_{st1} + c_1\dot{x}_{st1} - F_{antiroll1}$$

$$F_{z2} = k_2 \cdot x_{st2} + c_2\dot{x}_{st2} + F_{antiroll2}$$

$$F_{z3} = k3 \cdot x_{st3} + c_3\dot{x}_{st3} - F_{antiroll3}$$

$$F_{z4} = k_4 \cdot x_{st4} + c_4\dot{x}_{st4} + F_{antiroll4}$$

$$x_{st1} = z_{u1} - z - (t_f/2)\phi + a\theta$$

$$x_{st2} = z_{u2} - z + (t_f/2)\phi + a\theta$$

$$x_{st3} = z_{u3} - z - (t_r/2)\phi - b\theta$$

$$x_{st4} = z_{u4} - z + (t_r/2)\phi - b\theta$$

$$F_{antiroll1,2} = K_{arf}\phi/(t_f/2)$$

$$F_{antiroll3,4} = K_{arr}\phi/(t_r/2)$$

$$I_y\ddot{\theta} = -(F_{z1} + F_{z2})a + (F_{z3} + F_{z4})b \quad (2)$$

$$I_\phi\ddot{\phi} - h_s m_s V(\beta + \Psi) = -(F_{z1} - F_{z2})(t_f/2) + (F_{z3} - F_{z4})(t_r/2) + m_s g h_s \phi \quad (3)$$

The subsystems, as shown in Figs. (3) to (5), of full Simulink model are defined using the following:

$$mV(\beta + \Psi) - m_s h_s\ddot{\phi} = S_1 + S_2 + S_3 + S_4 \quad (4)$$

$$I_\Psi\ddot{\Psi} = (S_1 + S_2)a - (S_3 + S_4)b + M_{z1} + M_{z2} + M_{z3} + M_{z4} \quad (5)$$

$S_{1,2,3,4}$ and $M_{z1,2,3,4}$ denote cornering forces and aligning torque based on Fiala's formula which is a function of vertical load $W_{1,2,3,4}$ and slip angle $\beta_{1,2,3,4}$ as follows,

$$S_1 = \mu W_1(\lambda_1 - \lambda_1^2/3 + \lambda_1^3/27)$$

$$S_2 = \mu W_2(\lambda_2 - \lambda_2^2/3 + \lambda_2^3/27)$$

$$S_3 = \mu W_3(\lambda_3 - \lambda_3^2/3 + \lambda_3^3/27)$$

$$S_4 = \mu W_4(\lambda_4 - \lambda_4^2/3 + \lambda_4^3/27)$$

$$M_{z1} = -e\mu W_1(\lambda_1 - \lambda_1^2 + \lambda_1^3/3 - \lambda_1^4/27)$$

$$M_{z2} = -e\mu W_2(\lambda_2 - \lambda_2^2 + \lambda_2^3/3 - \lambda_2^4/27)$$

$$M_{z3} = -e\mu W_3(\lambda_3 - \lambda_3^2 + \lambda_3^3/3 - \lambda_3^4/27)$$

$$M_{z4} = -e\mu W_4(\lambda_4 - \lambda_4^2 + \lambda_4^3/3 - \lambda_4^4/27)$$

$$\lambda_1 = K_1\beta_1/(\mu W_1), \quad \lambda_2 = K_2\beta_2/(\mu W_2)$$

$$\lambda_3 = K_3\beta_3/(\mu W_3), \quad \lambda_4 = K_4\beta_4/(\mu W_4)$$

$$K_1 = p_1W_1^2 + q_1W_1, \quad K_2 = p_2W_2^2 + q_2W_2$$

$$K_3 = p_3W_3^2 + q_3W_3, \quad K_4 = p_4W_4^2 + q_4W_4$$

$$\beta_{1,2} = \delta - [(a\dot{\Psi} + V\beta)/V], \ \beta_{3,4} = [(b\dot{\Psi} - V\beta)/V]$$

$$\delta = \delta_{sw}/i_s \ , \ W_1 = \frac{W}{2}\left(\frac{b}{a+b}\right) + P_1$$

$$W_2 = \frac{W}{2}\left(\frac{b}{a+b}\right) + P_2 \ , \ W_3 = \frac{W}{2}\left(\frac{a}{a+b}\right) + P_3$$

$$W_4 = \frac{W}{2}\left(\frac{a}{a+b}\right) + P_4 \ , \ m_{u1}\ddot{Z}_{u1} = P_1 - F_{z1} \quad (6)$$

$$P_1 = k_{t1}x_{t1} = k_{t1}(z_{o1} - z_{u1})m_{u2}$$
$$\ddot{Z}_{u2} = P_2 - F_{z2} \quad (7)$$

$$P_2 = k_{t2}x_{t2} = k_{t2}(z_{o2} - z_{u2})m_{u3}$$
$$\ddot{Z}_{u3} = P_3 - F_{z3} \quad (8)$$

$$m_{u4}\ddot{Z}_{u4} = P_4 - F_{z4}$$
$$P_4 = k_{t4}x_{t4} = k_{t4}(z_{o4} - z_{u4}) \quad (9)$$

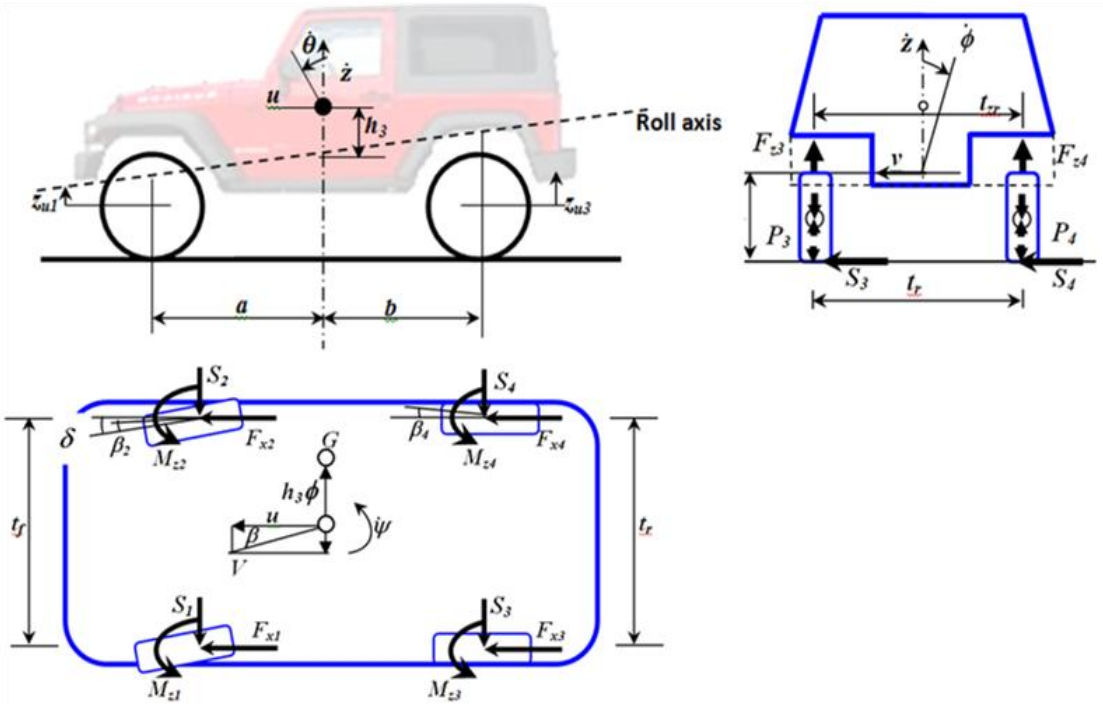

Fig. 1: Four wheeled full vehicle model

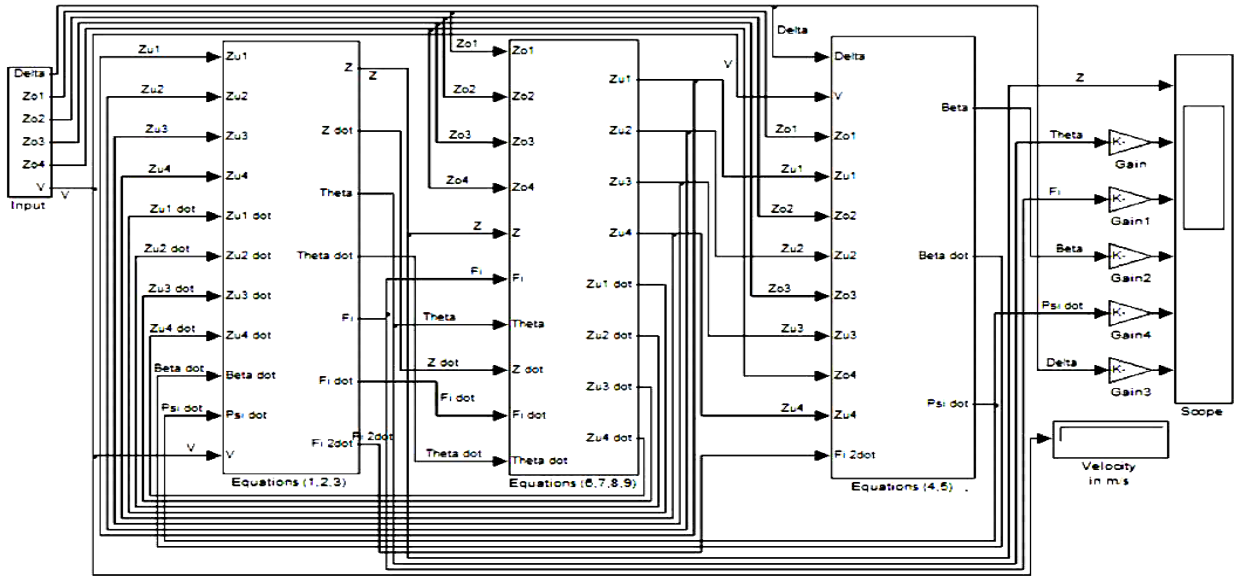

Fig. 2: Full vehicle Simulink model

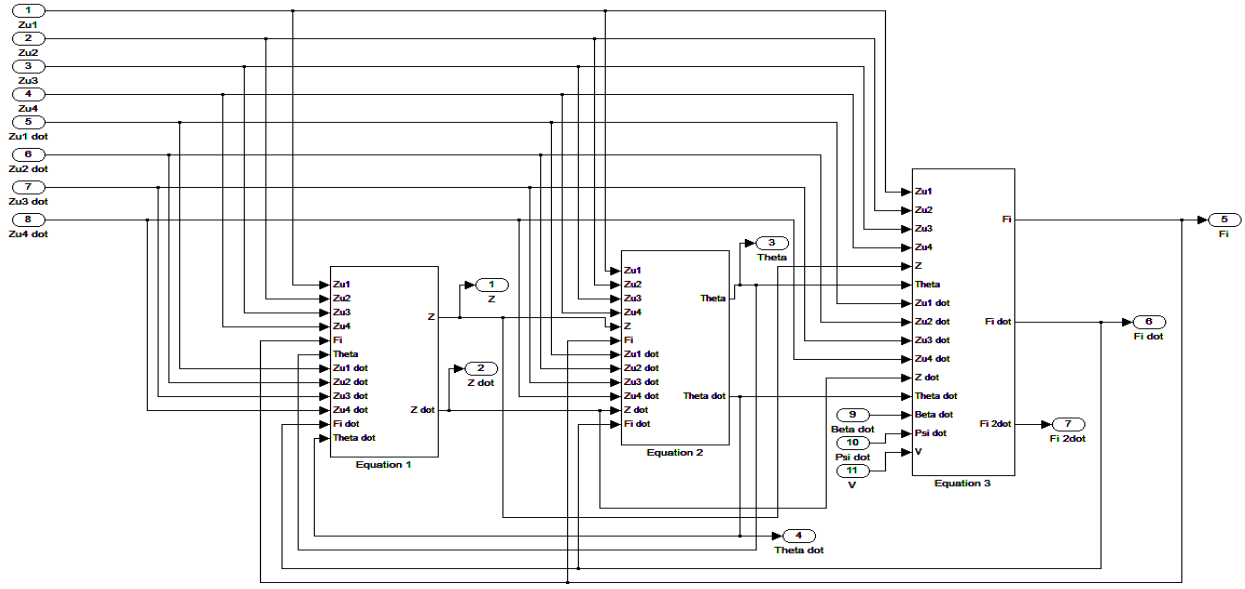

Fig. 3: Simulink subsystem for Eqns. (1) to (3)

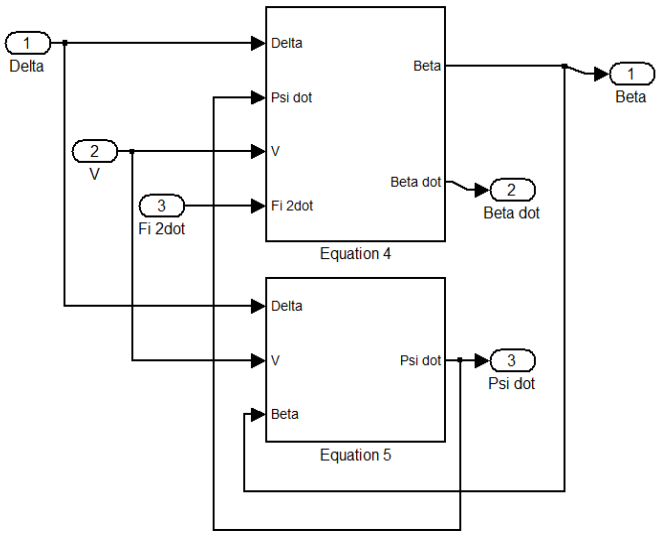

Fig. 4: Simulink subsystem for Eqns. (4) and (5)

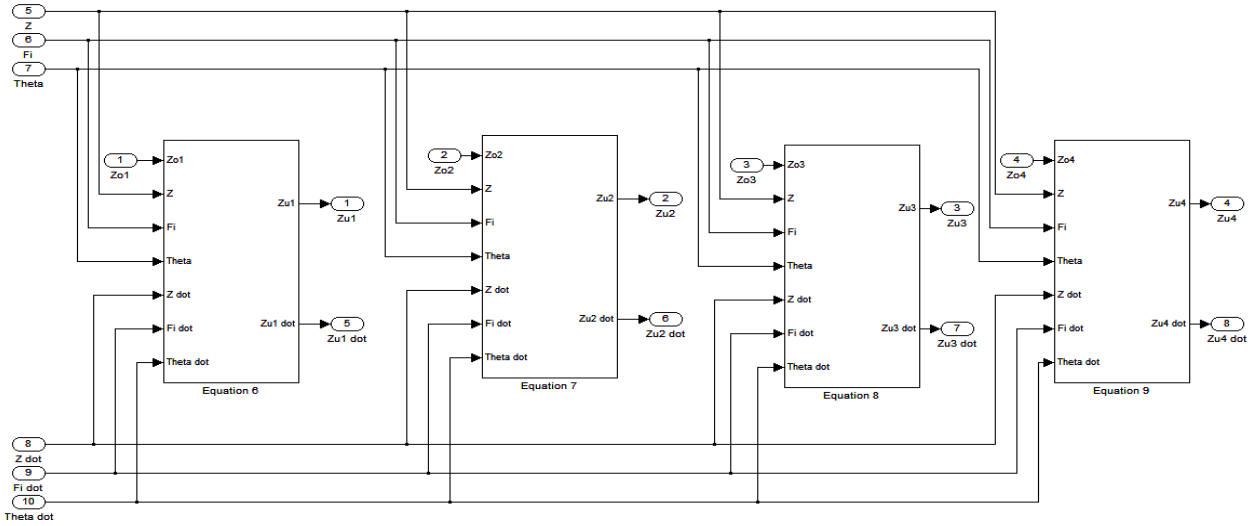

Fig. 5: Simulink subsystem for Eqns. (6) to (9)

Table 1: Mass properties used in the simulation

Symbol	Description	Value	Unit
M	Vehicle mass	1892	kg
m_s	Sprung mass	1562	kg
$m_{u1,2}$	Un-sprung mass	69	kg
$m_{u3,4}$	Un-sprung mass	96	kg
Iy	Pitch moment of inertia	1980	$kg.m^2$
Iϕ	Roll moment of inertia	1019	$kg.m^2$
Iψ	Yaw moment of inertia	3270	$kg.m^2$
$k_{1,2}$	Spring stiffness	27160	N/m
$k_{3,4}$	Spring stiffness	29420	N/m
$c_{1,2}$	Damping coefficient of damper	4000	N.s/m
$c_{3,4}$	Damping coefficient of damper	2500	N.s/m
Karf	Roll stiffness of anti-roll bar of the front	32400	N.m/rad
Karr	Roll stiffness of anti-roll bar of the rear	14100	N.m/rad
$k_{t1,2}$	Vertical stiffness of the front tire	229000	N/m
$k_{t3,4}$	Vertical stiffness of the rear tire	255000	N/m
A	Distance between center of gravity and front axle	1.34	m
B	Distance between center of gravity and rear axle	1.42	m
tf(r)	Wheel track	1.52	m
hs	Roll moment arm	0.62	m
E	Pneumatic trail	0.04	m
M	Friction coefficient	0.9	
G	Gravitational acceleration	9.81	m/s^2
pi	Constant	-0.0006	-
$q_{1,2}$	Constant	16.79	-
$q_{3,4}$	Constant	18.8	-
e	Constant	0.04	-
μ	Road friction coefficient	0.9	-

3. Results and discussions

Figs. 6, 7 and 8 show the effect of varied vehicle speeds from 80 km/hr to 120 km/hr on axle roll angle for slowly increasing steer angle. The first phase; from time 0 to 2 seconds, no additional torque is acting on the anti-roll bars, and accordingly the stiffness is equal. The vehicle is running in a steady state condition with constant roll angle, yaw rate, and constant slip angles. Since the slip angles at the front and rear ends are the same, the weight transfer on the front and rear axles are equal. In the second phase; an additional torque input is applied by causing an increase in the front weight and decrease in the rear weight. This creates a different steady state condition. The trend of roll angle curves for the systems with and without active anti-roll bars are the same and the maximum difference found at time 10 seconds. For side slip angle; the behaviour of the two systems was varied at the maximum time for all vehicle speeds. For the second phase on yaw rate curves, the trend of two systems with and without active anti-roll bars are the same and the maximum difference exists at 10 seconds in the opposite direction to roll and side slip angle. Reducing the front weight transfer causes increased force production capability on the front, while increasing the rear weight transfer decreased the grip in the rear, so the vehicle tends to have more over-steer behaviour. It is noted from the results that there is an improvement in

vehicle stability through the use of the effective roll control system compared with the passive system without control.

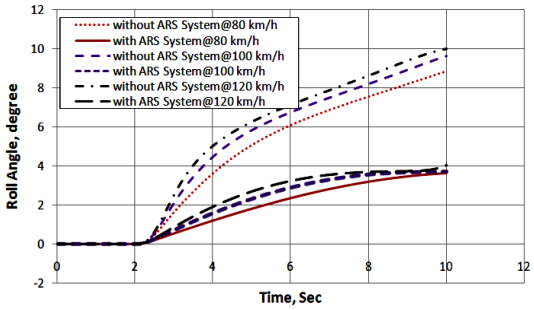

Fig. 6: Roll angle responses in step steer; slowly increasing steer

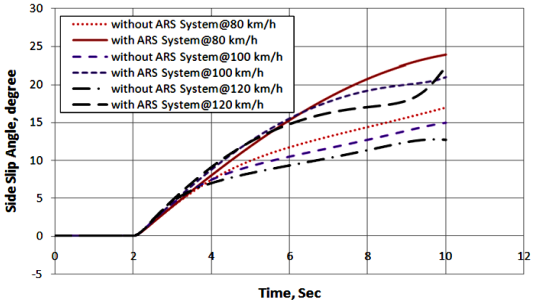

Fig. 7: Side slip angle resp. in step steer; slowly increasing steer

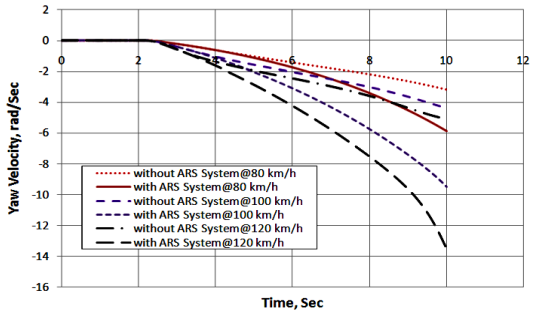

Fig. 8: Yaw velocity responses in step steer; slowly increasing steer

Figs. 9, 10 and 11 show the effect of vehicle speeds variation (from 80 km/hr to 120 km/hr) on axle roll angle, side slip angle, and yaw rate for step steer angle. First, there is no additional torque at the anti roll bars, so the stiffness is equal. In case the vehicle is running in a steady state condition with constant yaw rate and constant slip angles, the weight transfer on the front and rear axles is the same. In the second phase, an additional torque input is applied causing an increase in front weight transfer and decrease the in rear weight accordingly a different steady state condition is induced. This increase in front weight transfer causes reduced force production capability on the front. While decreasing the rear weight transfer increased the grip in the rear, so the vehicle tends to have a more under steer behaviour. This is shown by the decreased yaw rate and body slip angle. In the third phase of the model, the weight transfer on the front and rear is changed, by applying an opposite torque. In such situation, the rear end will lose grip and the vehicle will become instable. In the third phase (the steady state case), the roll angle starts at about 4 seconds, but the side slip angle and yaw rate start between 4 to 6 seconds.

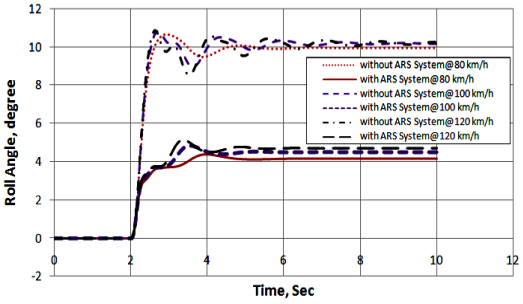

Fig. 9: Roll angle responses in step steer; step steer

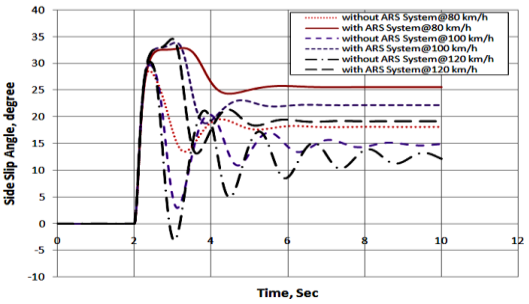

Fig. 10: Side slip angle responses in step steer; step steer

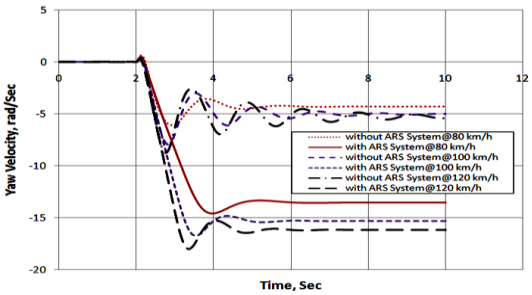

Fig. 11: Yaw velocity responses in step steer; step steer

The simulation results of body roll angle, side slip angle, and body yaw rate at the body center of gravity during double lane change at 80, 100 and 120 km/hr are shown in Figs. 12, 13 and 14 respectively. Double lane-change is a test that evaluates manoeuvrability of the vehicle. In real life, a double lane change often occurs when the driver is trying to avoid an accident. It can be concluded that controller with and without roll active system is able to improve significantly the ride performance compared to the passive system. Enhancement in ride performance may trim down the rate of driver fatigue and reduce the risk of the driver losing control of the vehicle.

J-turn manoeuvre is produced from a step steer input (δ = 3º). This manoeuvre represents a rapid transition from straight line running to constant radius cornering. Figs. 15, 16 and 17 show the time responses for a passive and controlled vehicle model for J-turn manoeuvre at 80km/hr to 120km/hr. In the passive vehicle, the normalized load transfers at the front and rear axles is > ±1. Moreover, the normalized load transfer builds up more quickly at the rear axle than at the front axle. In this situation, the inner wheels on the front and rear axles are without contact with the ground surface and the overturns of the vehicle. By using the active roll control, the normalized load transfer at the axles is approximately ≤ ±1. The vehicle rolls into the corner. This motion of the sprung mass generates stabilizing lateral displacement moment. The total roll

moment from the active anti-roll bars is distributed between the rear and front axles so that, as the lateral acceleration increases.

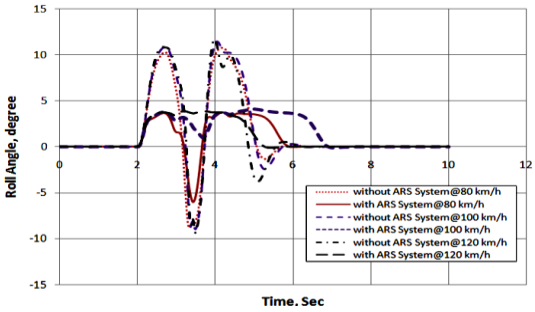

Fig. 12: Roll angle responses in step steer; double lane change

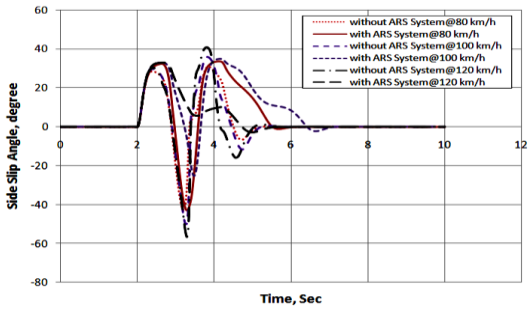

Fig. 13: Side slip angle responses in step steer; double lane change

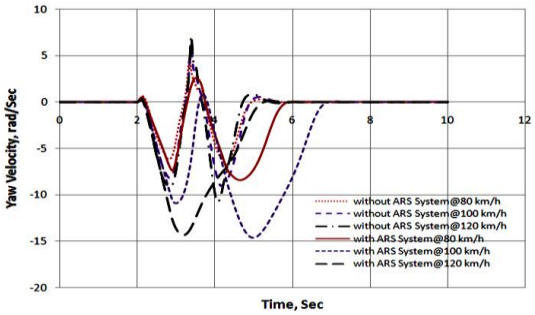

Fig. 14: Yaw velocity responses in step steer; double lane change

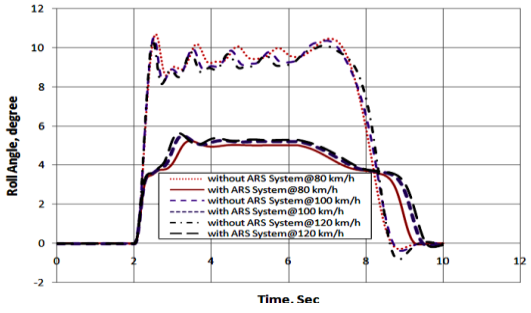

Fig. 15: Roll angle responses in step steer; J-turn

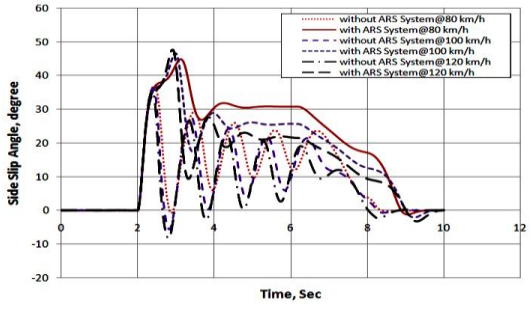

Fig. 16: Side slip angle responses in step steer; J-turn

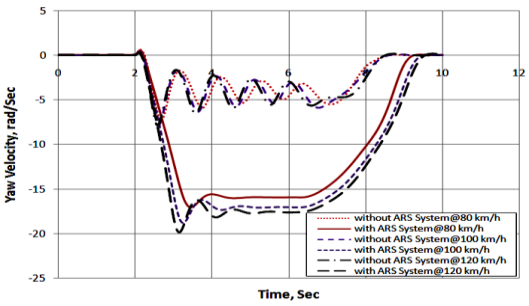

Fig. 17: Yaw velocity responses in step steer; J-turn

The fishhook manoeuvre is an important test in the context of rollover. It attempts to maximize the roll angle under transient conditions and is performed as follows, with a start speed of 80km/hr. The results obtained for the fishhook manoeuvre are shown in Figs. 18, 19 and 20 in terms of the maximum amplitude of steering angle, which can be applied without causing a rollover. Note that according to the definition of the amplitude for the fishhook manoeuvre, the maximum steering angle is actually 2 amplitudes. Thus the angle of 270° indicates that the vehicle cannot be rolled over in this manoeuvre. The maximum steering angle amplitude for the passive vehicle was 40°. All the remaining vehicles were able to negotiate this manoeuvre without rolling over regardless of the magnitude of the steering angle. The vehicle was more stable than with the active roll system. It exhibited consistently smaller vehicle side slip angles and no wheel lifts off, while the vehicle with the active roll system occasionally experienced one or two wheel lift off. In the case of fishhook manoeuvre, further simulations were conducted, in which the height of the center of gravity of the controlled vehicle was progressively raised, until the vehicle started to roll over at the same steering angle amplitude as the passive vehicle. It was found that presence of active roll system has shown an improvement in the vehicle resistance to manoeuvre-induced rollovers that is equivalent to increase in the static stability.

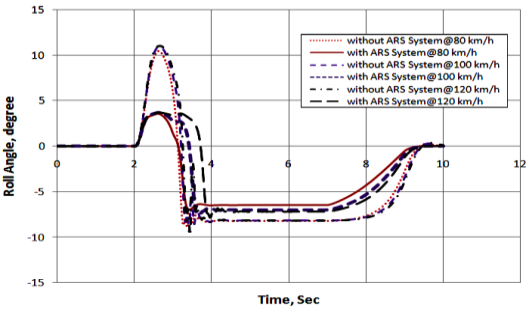

Fig. 18: Roll angle responses in step steer; fishhook

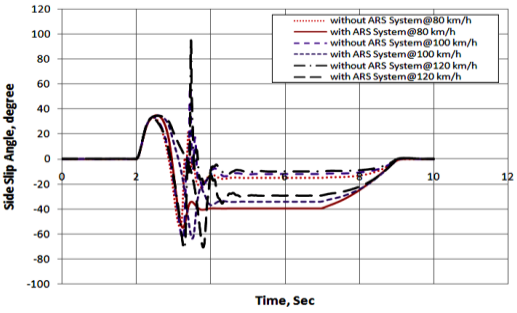

Fig. 19: Side slip angle responses in step steer; fishhook

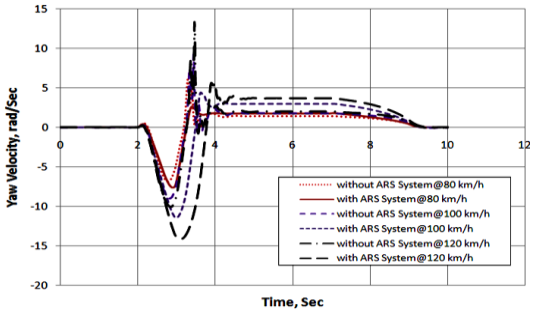

Fig. 20: Yaw velocity responses in step steer; fishhook

4. Conclusions

The results of the presented simulation model have shown a significance influence of the vehicle speed variation under different wheel steer angles (slowly increasing steer, step steer, double lane change, J-turn and fishhook) on roll angle, side slip angle and yaw rate. A comparison of the simulated passive and active anti-roll bar systems was also presented. The results showed that active roll stabilizer system achieved better roll angle reduction (about 40 to 60%) than passive anti-roll bar system having the same speed and step steer. The side slip angle of the active roll stabilizer system has increased (about 6 to 60%) than that of passive anti-roll bar system having the same speed and step steer. Fishhook manoeuvre has shown the highest value and the double lane change had the least increase. The results also showed an improvement in yaw velocity of the active roll stabilizer system approximately (15 to 60%) than the passive anti-roll bar system. Slowly increasing steer has the highest value and the fishhook has the least improvement. It is concluded that the simulated active roll stabilizer system can significantly improve the vehicle yaw stability when compared with passive one.

REFERENCES:

[1] P. Safi and M. Entezari. 2012. Fuzzy controller design for a novel vehicle rollover, prevention system, *Int. J. Machine Learning and Computing*, 2(5), 1-4.

[2] A.L. Svenson and A. Hac. 2004. Influence of chassis control systems on vehicle handling and rollover stability, *Proc. 19th Int. Tech. Conf. on the Enhanced Safety of Vehicles*, Washington.

[3] M. Krid and A.F. Ben. 2011. Design and control of an active anti-roll system for a fast rover, *Proc. IEEE/RSJ Int. Conf. Intelligent Robots and Systems*, San Francisco. https://doi.org/10.1109/IROS.2011.6094963.

[4] J.C. Dixon. 1996. *Tires, Suspension and Handling*, SAE International. https://doi.org/10.4271/R-168.

[5] H.B. Pacejka. 2002. *Tyre and Vehicle Dynamics*, Butterworth-Heinemann, Oxford.

[6] H. Rahnejat. 1998. *Multibody Dynamics: Vehicles, Machines, and Mechanisms*, SAE International.

[7] S. Hegazy, H. Rahnejat and K. Hussain. 1999. Multibody dynamics in full-vehicle handling analysis, *Proc. IMechE Part K: J. Multi-body Dynamics*, 213, 19-31. https://doi.org/10.1243/1464419991544027.

[8] S. Hegazy, H. Rahnejat and K. Hussain. 2000. Multibody dynamics in full-vehicle handling analysis under transient manoeuvre, *Vehicle Syst. Dyn.*, 34, 1-24. https://doi.org/10.1076/0042-3114(200008)34:1;1-K;FT001.

[9] M. Blundell and D. Harty. 2004. *Multibody Systems Approach to Vehicle Dynamics*, Butterworth-Heinemann, Oxford.

[10] R. Whitehead, W. Travis, D. Bevly and G. Flowers. 2004. A study of the effect of various vehicle properties on rollover propensity, *SAE Technical Paper 2004-01-2094*. https://doi.org/10.4271/2004-01-2094

[11] V. Drobny and M. Valasek. 2008. Vehicle lateral dynamics stabilization using active suspension, *Applied and Computational Mechanics*, 2, 255-264. https://doi.org/11025/1577.

[12] N. Sugimoto, S. Buma, S. Urababa and A. Nishihara. 2016. Electronic active stabilizer suspension system, development & realization, *Proc. JSME Mechanical Engineering*, Japan.

[13] Z. Kong, D. Pi, X. Wang, H. Wang and S. Chen. 2016. Design and evaluation of a hierarchical control algorithm for an electric active stabilizer bar system, *J. Mech. Engg.*, 62(10), 565-576. https://doi.org/10.5545/sv-jme.2016.3381.